The International Journal of

Robotics Research

Biological Cell Injection Using an Autonomous MicroRobotic System
Yu Sun and Bradley J Nelson

The online version of this article can be found at:

Multimedia Archives

Yu Sun
Bradley J. Nelson

Department of Mechanical Engineering
University of Minnesota
111 Church Street S.E.
Minneapolis, MN 55455, USA
yus@me.umn.edu

Biological Cell Injection Using an Autonomous MicroRobotic System

Abstract

Recent advances in microbiology, such as cloning, demonstrate that increasingly complex micromanipulation strategies are required for manipulating individual biological cells. In this paper, we present a microrobotic system capable of conducting automatic embryo pronuclei DNA injection (cell injection). Conventionally, cell injection has been conducted manually, however, long training, low success rates from poor reproducibility in manual operations, and contamination all call for the elimination of direct human involvement. To automate cell injections, a microrobotic system is developed that is capable of performing automatic embryo pronuclei DNA injection autonomously through a hybrid visual servoing control scheme. A Hough transform is used to detect the nuclei of embryos. Sum-of-squared-differences optical flow is used to track injection pipette motion, and auto focusing is implemented to determine the relative depth of subcellular structures. A hybrid control scheme is developed to fulfill the cell injection task. Upon the completion of injection, the DNA injected embryos are transferred into a pseudo-pregnant foster female mouse to reproduce transgenic mice for cancer studies. The experimental result shows that the injection success rate is 100%.

KEY WORDS—microrobotic system, cell injection, visual servoing, position control

1. Introduction

The ability to analyze individual cells rather than averaged properties over a population is a major step towards understanding the fundamental elements of biological systems. Studies of single cells are a key component in the development of highly selective cell-based sensors, the identification of genes, bacterial synthesis of specific DNA, and certain approaches to gene therapies. Treatments for severe male infertility and the production of transgenic organisms require that individual cells are isolated and individually injected. These

recent advances in microbiology as well as other significant research efforts, such as cloning, demonstrate that increasingly complex micromanipulation strategies are required for manipulating individual biological cells.

Microrobotics and microsystems technology can play important roles in manipulating cells, a field referred to as biomanipulation. In this paper, we present a visually servoed microrobotic system capable of performing automatic pronuclei DNA injection, which is a method for introducing DNA into embryos in order to create transgenic organisms. In Figure 1, a holding pipette holds a mouse embryo and an injection pipette performs the injection task. The objective of pronuclei injection is, in this case, to produce transgenic mice for use in cancer studies.

Conventionally, cell injection is conducted manually. Operators often require at least a year of full-time training to become proficient at the task, and success rates are often disappointingly low. One reason for this is that successful injections are not precisely reproducible. A successful injection is determined greatly by injection speed and trajectory (Kimura and Yanagimachi 1995). Automated cell injection can be highly reproducible with precision control of pipette motion. The second reason for the low success rate of conventional cell injection is due to contamination. This also calls for the elimination of direct human involvement. Therefore, the main advantages of automated cell injection are that it reduces the need for extended training, reduces the risk of contamination, and is highly reproducible which greatly increases the success rate.

The autonomous microrobotic system described in this paper is developed to conduct autonomous pronuclei DNA injection of mouse embryos. A hybrid control scheme is developed to fulfill the cell injection task. The nuclei are detected automatically. A sum-of-squared-differences optical flow (SSD) tracking algorithm is adopted for visual servoing. Auto focusing is implemented by template matching. Upon the completion of injection, the DNA injected embryos are transferred into the ampulla of a pseudo pregnant foster female mouse
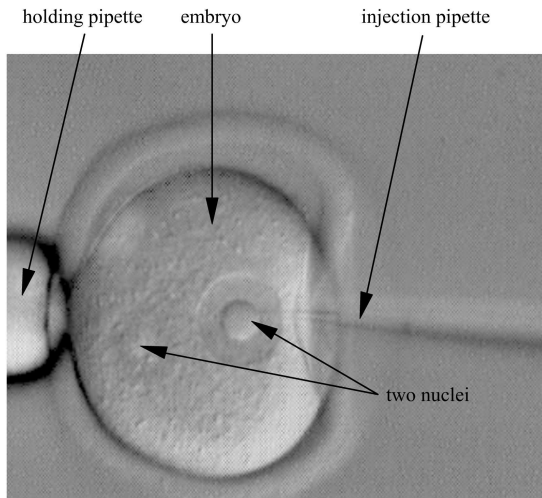
861

holding pipette   embryo   injection pipette

two nuclei

Fig. 1. Cell injection of a mouse embryo. The embryo is approximately 55 μm in diameter.

to reproduce transgenic mice. Results show that the injection success rate is 100%.

2. Biomanipulation

Biomanipulation entails such operations as positioning, grasping, and injecting material into various locations in cells. Existing biomanipulation techniques can be classified as non-contact manipulation including laser trapping (Ashkin 1970; Ashkin, Dziedzic, and Yamane 1987; Ashkin and Dziedzic 1987; Bruican et al. 1987; Wright et al. 1990; Conia, Edwards, and Voelkel 1997) and electro-rotation (Washizu et al. 1993; Washizu and Jones 1996; Nishioka et al. 1997; Arai et al. 1997), and contact manipulation referred to as mechanical micromanipulation (Kimura and Yanagimachi 1995). When laser trapping is used for non-contact biomanipulation, a laser beam is focused through a large numerical aperture objective lens, converging to form an optical trap in which the lateral trapping force moves a cell in suspension toward the center of the beam. The longitudinal trapping force moves the cell in the direction of the focal point. The optical trap levitates the cell and holds it in position. Laser traps can work in a well-controlled manner. However, the high dissipation of visible light in aqueous solutions requires the use of high-energy light close to the ultraviolet (UV) spectrum, raising the possibility of damage to the cell. Even though some researchers claim that such concerns could be overcome using wavelengths in the near-infrared (NIR) spectrum (Conia, Edwards, and Voelkel 1997; Ponelies et al. 1994), there is still the question as to whether the incident laser beam might induce abnormalities in the cells' genetic material. One alternative to using laser beams is the electro-rotation technique. Electric-field-induced rotation of cells was demonstrated by

Washizu et al. (1993), Arnold and Zimmermann (1988) and Mischel, Voss, and Pohl (1982), and using the dielectrophoresis (DEP) effect to manipulate cells was reported by Fuhr et al. (1994). This non-contact cell manipulation technique is based on controlling the phase shift and magnitude of electric fields. These fields, appropriately applied, produce a torque on the cell. Different system configurations have been established for cell manipulation based on this principle (Nishioka et al. 1997; Arai et al. 1997), which can achieve high accuracy in cell positioning. However, this technique lacks a means to hold the cell in place for further manipulation, such as injection, since the magnitude of the electric fields has to be kept low to ensure the viability of cells. The damage caused by laser beams in the laser trapping technique and the lack of a holding mechanism in the electro-rotation technique can be overcome by mechanical micromanipulation.

Mechanical micromanipulation is a technique for extending human manual capabilities, which are naturally restricted to certain tolerances. In automatically manipulating biological cells or microassembling microcomponents, high-precision actuators such as piezoelectric driven micromanipulators are often adopted (Carrozza et al. 1998; Santa, Mews, and Riedmiller 1998). These microrobots must be specially designed for different applications.

Many research efforts in biomanipulation stress positioning and grasping cells, however most current microactuators that are based on electrostatic, thermal, magnetic, or pneumatic principles are not suitable for operation in liquid surroundings. In order to capture cells in liquids, several micromachined actuators have been developed. These include a pneumatic microactuator insulated by a microcage (Ok, Chu, and Kim 1999), conjugated polymers (Smela 1999), and a Nafion actuator (Li et al. 2000). Even though these microactuators can fulfill cell capturing tasks, they are not capable of performing cell injection.

In the autonomous cell injection system described in this paper, a general-purposed three-degrees-of-freedom (3-DoF) microrobot is used. Commercially available micropipettes that are well suited for functioning as end-effectors in liquids are mounted on the microrobot. To make the cell injection system operate autonomously, automatic nuclei detection and visual servoing are implemented. A hybrid controller integrating visual servoing and precision position control is developed. Because focusing takes significant time and efforts during manual operations, automatic focusing is also implemented.

3. Mouse Embryo Preparation

The embryos used in the experiments are collected in the Cancer Center at the University of Minnesota in accordance with standard embryo preparation procedure (Hogan et al. 1994). Three-week-old FVB/N female mice are injected with pregnant mare serum (PMS) to promote oval maturation. After

approximately 45 h, the mice are injected with human chorionic gonadotropin (hCG) to promote synchronized ovulation. Then the superovulated female mice are mated to fertile male mice. Finally, embryos are collected from the ampulla of female mice. A typical embryo is shown in Figure 1. The average diameter of the embryos is 55 μm.

4. System Setup

The autonomous embryo injection system is composed of an injection unit, an imaging unit, a vacuum unit, and a software unit. The system setup is shown in Figure 2.

For embryo injection vibration must be well controlled. Vibration not only causes difficulty in visually tracking features but also produces permanent and fatal harm in the injected location and the surrounding area. To minimize vibration, all units except the host computer and the vacuum units of the embryo pronuclei DNA injection system are mounted on a floating table.

4.1. Injection Unit

The injection unit of the system includes a holding pipette, an injection pipette, two standard pipette holders, a high precision 3-DoF microrobot, and a coarse manipulator.

The injection and holding pipettes are both processed using a micropipette puller. The dimensions of the pipette tips are 1 μm in inner diameter for the injection pipettes and 20 μm in outer diameter for the holding pipettes. Both the holding pipettes and injection pipettes are held by pipette holders.

Extremely high-precision motion control is required for successful embryo injection. A 3-DoF microrobot is used in which each of the XYZ axes has a travel of 2.54 cm with a step resolution of 40 nm. An injection pipette with a pipette holder is installed on the microrobot, as shown in Figure 3.

The holding pipette is installed on a micromanipulator that is a manually operated three-dimensional (3D) coarse manipulator. The holding pipette holder and the injection pipette holder are both connected with Teflon tubing such that negative and positive pressure are provided to the tips of the pipettes for holding embryos and depositing DNA.

4.2. Imaging Unit

The imaging unit of the embryo injection system includes an inverted microscope, a CCD camera, a PCI framegrabber, and a host computer. An inverted microscope is used with a 400$\times$ objective. The CCD camera is mounted on the port of the microscope. The framegrabber captures thirty frames per second. The tracking of image features, which is required for semi-autonomous teleoperation and autonomous injection, is performed on the host computer (a 450 MHz Celeron processor) at 30 Hz.
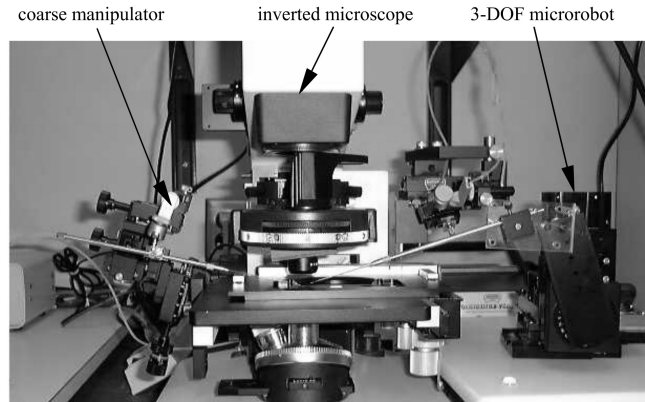
coarse manipulator   inverted microscope   3-DOF microrobot

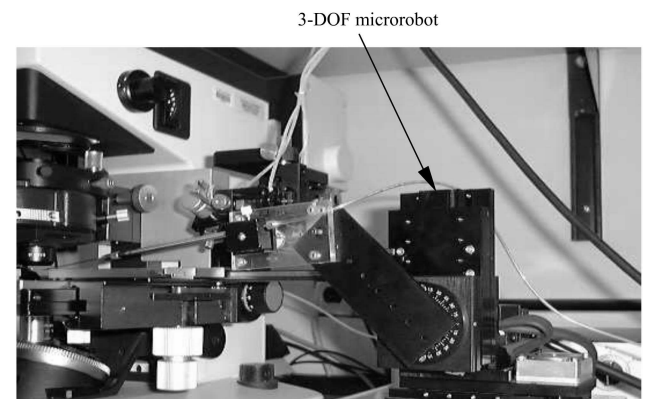Fig. 2. Autonomous embryo injection system.

3-DOF microrobot

Fig. 3. 3-DoF high-precision microrobot with a mounted micropipette.

5. Embryo Injection

5.1. Teleoperated Embryo Injection

The system is first developed for operating in a teleoperation mode. A supervisor guides a cursor on a monitor (using a computer mouse) which the visual servoing system accepts as a control input to a visual servoing control law. Figure 4 shows the program interface that performs teleoperated injection.

The main teleoperation injection process flow is described as follows:

Step 1. focus on the nucleus of the embryo;

Step 2. servo the tip of the injection pipette, bringing it into focus;

Step 3. control the vacuum unit to hold the embryo;

Step 4. guide the injection pipette to the edge of the embryo, well aligned with the larger nucleus of the embryo;

Step 5. control the injection pipette to move into the nucleus of the embryo;

Fig. 4. Teleoperated embryo injection.

Step 6. deposit DNA inside the nucleus of the embryo;

Step 7. move the injection pipette out of the embryo. This completes the teleoperation process.

As shown above, a supervisor is required to guide the injection pipette's motion. First, the supervisor locates the nucleus where the injection pipette will be guided. Secondly, the supervisor decides where the injection pipette should stop inside the embryo. Thirdly, the supervisor controls the speed of the injection pipette. For example, the injection pipette must be moved inside the embryo at a low speed, while it must be extracted from the embryo after injection at a much higher speed, which is a significant factor in improving the injection success rate. To make the system operate in an autonomous mode without the intervention of a supervisor, an autonomous embryo injection system is developed.

5.2. Automatic Embryo Injection

Automatic embryo injection begins with identifying one of the nuclei by using a Hough transform. Once the nucleus is located, the microrobot carrying the injection pipette is guided to the edge of the nucleus. In this process, SSD tracking is used for tracking the movement of the injection pipette. When the injection pipette moves inside the embryo, the control scheme is switched from visual servoing to position control, which is described in detail in Section 5.2.3.

5.2.1. Detection of the Nucleus and Switching Point

The Hough transform is a powerful technique for isolating features of a particular shape within an image. The transform is implemented by quantizing the Hough parameter space into

finite intervals or accumulator cells. In our experiments, the feature of interest is one of the circle-shaped nuclei shown in Figure 6. As described by the parametric equation for circles $(x - a)^2 + (y - b)^2 = r^2$, there are three parameters to be detected: a and b refer to the center position, and r represents the circle radius. The computational requirements of a 3D Hough transform are avoided in the detection of nuclei because the nuclei are always approximately 10 μm in diameter. Figure 6(a) shows a detected nucleus. This provides the visual control system with the target destination where the injection pipette is guided.

The outer membrane of the embryo is detected in a similar manner. The switching area discussed in Section 5.2.3 is chosen such that its center is located on the edge of the outer membrane while having the same Y coordinate as the detected nucleus.

5.2.2. SSD Tracking Algorithm

For tracking the movement of the injection pipette for visual servoing, the SSD tracking algorithm is used (Nelson, Papanikolopoulos, and Khosla 1993; Papanikolopoulos 1995). SSD is an effective method for tracking in a structured environment where image patterns do not change considerably between successive frames of images. In visually servoing a microrobot under a microscope, the predictable environment and controlled illumination make SSD a robust tracking method. It is desirable to select features with high gradients, such as edges and corners that are distinct from their neighboring regions. In embryo injections, the tip of the injection pipette is selected as a feature. In general, brightness patterns can be represented by three variables: two space variables x and y, and a time variable t, as $Image(x, y, t)$. The basic assumption of SSD tracking is that intensity patterns $Image(x, y, t)$ in a sequence of images do not change rapidly between successive images. In implementing the algorithm, a template of 20×20 pixels around the feature is acquired that is the tip of the injection pipette. An SSD correlation measure is calculated for each possible displacement (dx, dy) within a search window in the updated image $Image(x, y, t + 1)$:

$$SSD(dx, dy) = \sum_{i,j \in N} [Image(x_1 + dx + i, y_1 + dy + j) \\ - Template(x_1 + dx + i, y_1 + dy + j)]^2.$$

(1)

The distance (dx, dy) having the minimum SSD measure in equation (1) is assumed to be the displacement of the feature. The amount of processing depends greatly on the template size and the size of the search window. A large template will increase robustness, while a larger search window will handle larger displacements, provided frames of images can be processed in real time. In the implementation, a search window of 40×40 pixels is acquired.

5.2.3. Hybrid Control Scheme for Embryo Injection

The hybrid control scheme consists of image-based visual servoing and precision position control. In image-based visual servoing, the error signal is defined directly in terms of image feature parameters. The motion of the microrobot causes changes to the image observed by the vision system. Although the error signal is defined in the image parameter space, the microrobot control input is typically defined either in joint coordinates or in task space coordinates. In formulating the visual servoing system, task space coordinates are mapped into sensor space coordinates through a Jacobian mapping. Let x_T represent coordinates of the end-effector of the microrobot on the task space, and $\dot{x}_T$ represent the corresponding end-effector velocity. Let x_I represent a vector of image feature parameters and $\dot{x}_I$ the corresponding vector of image feature parameter rates of change. The image Jacobian, $J_v(x_T)$, is a linear transformation from the tangent space of task space T at x_T to the tangent space of image space I at x_I.

$$\dot{x}_I = J_v(x_T)\dot{x}_T \tag{2}$$

where $J_v(x_T) \in \Re^{k \times m}$, and

$$J_v(x_T) = \left[\frac{\partial x_I}{\partial x_T} \right]$$

$$= \begin{bmatrix} \frac{\partial x_{I1}(x_T)}{\partial x_{T1}} & \cdots & \frac{\partial x_{I1}(x_T)}{\partial x_{Tm}} \\ \cdots & \cdots & \cdots \\ \frac{\partial x_{Ik}(x_T)}{\partial x_{T1}} & \cdots & \frac{\partial x_{Ik}(x_T)}{\partial x_{Tm}} \end{bmatrix}. \tag{3}$$

k is the dimension of the image feature parameter space; and m is the dimension of the task space T.

The state equation for the visual servoing system is as follows

$$x(k+1) = x(k) + \frac{1}{f} J_v(k)u(k) \tag{4}$$

where $x(k) \in \Re^{2M}$ (M is the number of features being tracked), f is the sampling frequency of the vision system, and $u(k) = \begin{bmatrix} \dot{X}_T & \dot{Y}_T \end{bmatrix}$ is the microrobot's end-effector velocity.

The control objective of the system is to control the motion of the end-effector, i.e., the injection pipette, in order to place the image plane coordinates of the feature on the target in the switching area shown in Figure 6(a). The control strategy used to achieve the control objective is based on the minimization of an objective function that places a cost on errors in feature positions, $[x(k+1) - x_{switch}]$, and a cost on providing a visual control input $u(k)$:

$$E(k+1) = [x(k+1) - x_{switch}]^T Q [x(k+1) - x_{switch}]$$

$$+ u^T(k)Lu(k). \tag{5}$$

This expression is minimized with respect to the current control input $u(k)$. The result is the following expression for the control input:

$$u(k) = -\left[\frac{1}{f} J_v^T(k)Q\frac{1}{f} J_v(k) + L \right]^{-1}$$

$$\frac{1}{f} J_v^T(k)Q [x(k) - x_{switch}]. \tag{6}$$

The weighting matrices $Q \in \Re^{k \times k}$ and $L \in \Re^{m \times m}$ allow the user to place more or less emphasis on the feature error and the control input. Extensions to this system model and control derivations that account for system delays, modeling and control inaccuracy, and measurement noise have been experimentally investigated (Papanikolopoulos, Nelson, and Khosla 1992).

When the visual servoing controller guides the end-effector of the microrobot into the switching area that is of the same Y coordinate as the nucleus detected using a Hough transform, the control scheme switches to precision position control. Visual servoing and precision position control jointly form the hybrid control scheme for automatic embryo pronuclei DNA injection. The complete hybrid control scheme is

$$U(k) = F_\sigma \begin{bmatrix} x(k) - x_{switch} \\ x_T(k) - x_{TD} \end{bmatrix} \tag{7}$$

where

$$F_\sigma = \begin{bmatrix} \left(-\sigma_1 \left[\frac{1}{f} J_v^T(k)Q\frac{1}{f}J_v(k) + L \right]^{-1} \frac{1}{f} J_v^T(k)Q \right)^T \end{bmatrix}^T \\ \sigma_2 I \end{bmatrix}. \tag{8}$$

I is a 2×2 identity matrix; and x_{TD} is the desired position on the task space T.

The switching condition is $\sigma_1\sigma_2 = 0$, and

$$\begin{aligned} \sigma_1 &= 1 \quad \text{when} \quad x(k) \notin (c, r) \\ \sigma_2 &= 1 \quad \text{when} \quad x(k) \in (c, r) \end{aligned}$$

where (c, r) is the switching area shown in Figure 6(a).

Figure 5 shows the block diagram of the hybrid control system for embryo pronuclei DNA injection. The hybrid controller $c_{switch}(t)$ selects the controller in the hybrid control system based on visual feedback and the switching conditions.

The injection pipette is originally positioned away from the embryo shown in Figure 6(a). The nucleus is detected using a Hough transform which provides the target destination in the horizontal direction. The hybrid controller guides the microrobot with the injection pipette into the nucleus of the embryo where DNA is deposited. Figure 6(b) shows the injection process.
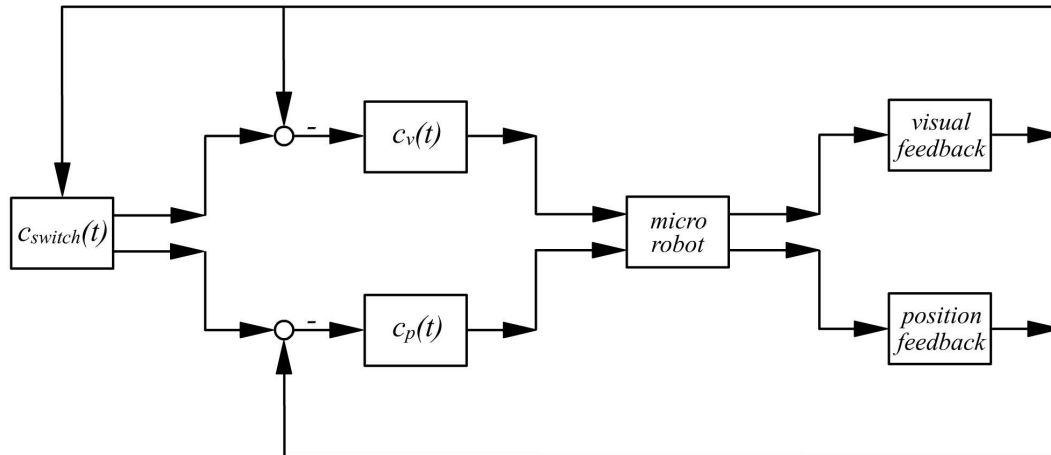
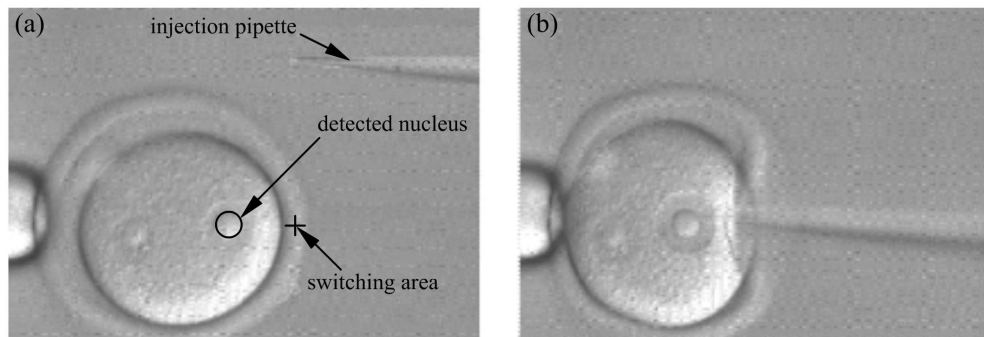Fig. 5. Hybrid control scheme for embryo pronuclei DNA injection.

Fig. 6. Embryo pronuclei DNA injection using hybrid control.

6. Automatic Focusing

For embryo pronuclei DNA injection, focusing must be performed precisely on the central plane of one of the two nuclei, the tip of the holding pipette, and the tip of the injection pipette. Failure to do so will cause the injection pipette to "slide" over the top of the embryo, failing to puncture the nucleus membrane, and possibly causing serious injury to the cell membrane. This makes precise focusing important.

In the experiments conducted, each batch of oocytes consisting of approximately ten egg cells is loaded from the incubator onto slides. Unloading and reloading cannot be completed unless the injection pipettes are moved out of focus and back into focus. In addition, when switching among the ten cells in one batch, the injection pipette must be moved out of the focus plane and brought back into focus before injection is conducted. Refocusing takes significant time and effort during manual operations, which makes automatic focusing important.

Defocus acts as a low-pass filter that attenuates high-frequency content in an image (Born and Wolf 1965; Horn 1986). The level of focus in an image can thus be estimated by computing the frequency content in an image. Various focus measures and metrics have been proposed and developed in the past, such as Fourier transform (Bove 1989), Tenengrad (Schlag et al. 1983), high-pass filtering and modified Laplacians (Nayar and Nakagawa 1990; Noguchi and Nayar 1996), histogram entropy (Schlag et al. 1983), and gray-level variance and sum-modulus difference (Nahaniel, Neow, and Ang 2001).

In this application, since the injection pipette only needs to be moved in a plane perpendicular to the platform of the microscope when switching among cells or among batches, automatic focusing can be implemented by using a simple template matching technique.

The error between pixel values in the template and the image is minimized when the injection pipette is in the focus plane. Figure 7 shows the change of the error with the distance
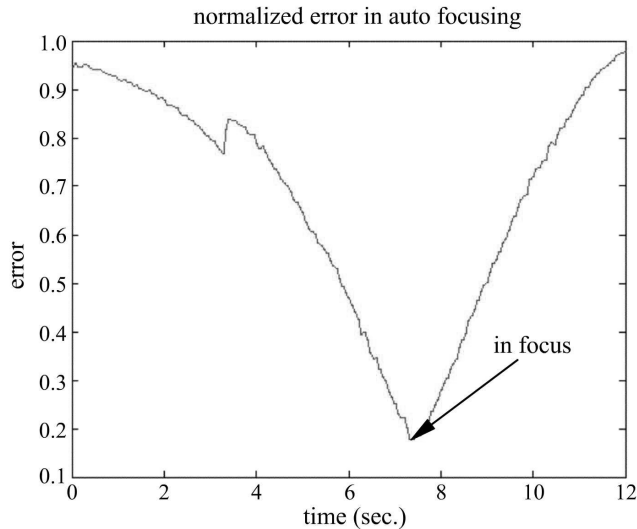
Fig. 7. Error change in automatic focusing.

between each position of the injection pipette and the focus plane. Templates can be obtained while the injection pipettes are initially in focus. After switching among cells or batches, the microrobot controls the injection pipette to move down, performing template matching to guide the pipettes into focus. Experimental results demonstrate that this technique provides satisfactory performance.

7. Experimental Results

Experimental results demonstrate that the hybrid control scheme for autonomous cell injection is successful. Nuclei detection and auto focusing operate with robustness. Visual servoing and precision motion control are switched successfully in the complete hybrid controller.

Eight mouse embryos were collected for embryo pronuclei DNA injection. Three of the eight embryos were discarded due to abnormalities in the nuclei. The autonomous injection microrobotics system continuously conducted embryo pronuclei DNA injection on the five selected embryos. All five injected embryos proved to be viable and were transferred into a foster female mouse to reproduce transgenic mice. In nineteen days, transgenic mice were reproduced. Experimental results demonstrate that the success rate for automatic injection is 100%. This compares quite favorably with manual injection success rates, which are estimated by injection technicians to have success rates of approximately 20–80%. The time required to perform the injections is comparable with manual operation by a proficient technician.

8. Conclusions

An autonomous embryo pronuclei DNA injection system was developed. Visual servoing and precision motion control were combined into the hybrid control scheme. A Hough transform was used to detect the nuclei of the embryos, which provides the target destination for the visual servoing control system. Precise auto focusing was implemented for the autonomous cell injection system. Experimental results show that the success rate for embryo pronuclei DNA injection is 100%. The complete system demonstrates that microrobotics technology can play important roles in automating and facilitating biomanipulation tasks.

Further enhancement of the system will integrate a cell capturing subsystem on the holding micropipette side to fully automate the injection process. The incorporation of force feedback (Kimura and Yanagimachi 1995) will improve injection speeds and will also allow researchers to more fully characterize cell membrane properties further improving general cell injection techniques.

Appendix: Index to Multimedia Extensions

The multimedia extension page is found at http://www.ijrr.org.

Table of Multimedia Extensions

Extension	Type	Description
1	Video	Autonomous microrobotic cell injection process

Acknowledgments

References

Arai, F., Morishima, K., Kasugai, T., and Fukuda, T. 1997. Bio-Micromanipulation (new direction for operation improvement). In *Proceedings of the 1997 IEEE/RSJ International Conference on Intelligent Robot and Systems, IROS 1997*, Grenoble, France, 7–11 September 1997, pp. 1300–1305.

Arnold, W. M., and Zimmermann, U. 1988. Electro-rotation: development of a technique for dielectric measurements on individual cells and particles. *Journal of Electrostatics* 21(2–3):151–191.

Ashkin, A. 1970. Acceleration and trapping of particles by radiation pressure. *Physical Review Letters* 24(4):156–159.

Ashkin, A., and Dziedzic, J. M. 1987. Optical trapping and manipulation of viruses and bacteria. *Science* 235(4795):1517–1520.

Ashkin, A., Dziedzic, J. M., and Yamane, T. 1987. Optical trapping and manipulation of single cells using infrared laser beams. *Nature* 330(24–31):769–771.

Born, M., and Wolf, E. 1965. *Principles of Optics: Electromagnetic Theory of Propagation, Interference and Diffraction of Light*, Pergamon, London.

Bove Jr., M. V. 1989. Discrete Fourier transform based depth-from-defocus. *Image Understanding and Machine Vision 1989, Technical Digest Series 14 Conference edition*, pp. 118–121.

Bruican, T. N., Smyth, M. J., Crissman, H. A., Salzman, G. C., Stewart, C. C., and Martin, J. C. 1987. Automated single-cell manipulation and sorting by light trapping. *Applied Optics* 26(24):5311–5316.

Carrozza, M. C., Dario, P., Menciassi, A., and Fenu, A. 1998. Manipulating biological and mechanical micro-objects using LIGA-microfabricated end-effectors. In *Proceedings of the 1998 IEEE International Conference on Robotics and Automation, ICRA 1998*, Leuven, Belgium, May 1998, pp. 1811–1816.

Conia, J., Edwards, B. S., and Voelkel, S. 1997. The micro-robotic laboratory: optical trapping and scissing for the biologist. *Journal of Clinical Laboratory Analysis* 11(1):28–38.

Fuhr, G., Muller, T., Schnelle, T., Hagedorn, R., Voigt, A., Fiedler, S., Arnold, W. M., Zimmerman, U., Wagner, B., and Heuberger, A. 1994. Radio frequency microtools for particle and live cell manipulation. *Naturwissenschaften* 81(12):528–535.

Hogan, B., Beddington, R., Costantini, F., and Lacey, E. 1994. *Manipulating the Mouse Embryo: A Laboratory Manual*, 2nd edition, Cold Spring Harbor Laboratory Press.

Horn, B. K. P. 1986. *Robot Vision*, MIT Press.

Kimura, Y., and Yanagimachi, R. 1995. Intracytoplasmic sperm injection in the mouse. *Biology of Reproduction* 52(4):709–720.

Li, W. J., Kwok, Y. F., Qin, S. J., and Xu, Y. S. 2000. Micro nafion actuators for cellular motion control and underwater manipulation. In *Proceedings of the 7th International Symposium on Experimental Robotics, ISER 2000*, Hawaii, 10–13 December 2000, pp. 463–473.

Mischel, M., Voss, A., and Pohl, H. A. 1982. Cellular spin resonance in rotating electric fields. *Journal of Biological Physics* 10(4):223–226.

Nathaniel, N. K. C., Neow, P. A., and Ang Jr., M. H. 2001. Practical issues in pixel-based autofocusing for machine vision. In *Proceedings of the 2001 IEEE International Conference on Robotics and Automation, ICRA 2001*, Seoul, Korea, 21–26 May 2001, Vol. 3, pp. 2791–2796.

Nayar, H. K., and Nakagawa, Y. 1990. Shape from focus: an effective approach for rough surfaces. In *Proceedings of the 1990 IEEE International Conference on Robotics and Automation, ICRA 1990*, Cincinnati, OH, 13–18 May 1990, Vol. 2, pp. 218–225.

Nelson, B. J., Papanikolopoulos, N. P., and Khosla, P. K. 1993. Visual servoing for robotic assembly. In *Visual Servoing*, World Scientific Series in Robotics and Automation, Vol. 7, pp. 139–164.

Nishioka, M., Katsura, S., Hirano, K., and Mizuno, A. 1997. Evaluation of cell characteristics by step-wise orientational rotation using optoelectrostatic micromanipulation. *IEEE Transactions on Industry Applications* 33(5):1381–1388.

Noguchi, M., and Nayar, H. K. 1996. Microscopic shape from focus using a projected illumination pattern. *Journal of Mathematical Computer Modeling* 24(5–6):31–48.

Ok, J., Chu, M., and Kim, C. J. 1999. Pneumatically driven microcage for micro-objects in biological liquid. In *Proceedings of the 12th IEEE International Conference on Micro Electro Mechanical Systems, MEMS 1999*, Orlando, FL, 17–21, January 1999, pp. 459–463.

Papanikolopoulos, N. P. 1995. Selection of features and evaluation of visual measurements during robotic visual servoing tasks. *Journal of Intelligent and Robotic Systems: Theory and Applications* 13:279–304.

Papanikolopoulos, N. P., Nelson, B. J., and Khosla, P. K. 1992. Full 3-D tracking using the controlled active vision paradigm. In *Proceedings of the 1992 IEEE International Symposium on Intelligent Control*, Glasgow, Scotland, 11–13 August 1992, pp. 267–274.

Ponelies, N., Scheef, J., Seeger, S., and Greulich, K. O. 1994. Laser micromanipulators for biotechnology and genome research. *Journal of Biotechnology* 35:109–120.

Santa, K., Mews, M., and Riedmiller, M. 1998. Neural approach for the control of piezoelectric micromanipulation robots. *Journal of Intelligent and Robotic Systems* 22(3–4):351–374.

Schlag, J. F., Sanderson, A. C., Neumann, C. P., and Wimberly, F. C. 1983. Implementation of automatic focusing algorithms for a computer vision system with camera control. *Technical Report*, CMU-RI-TR-83-14.

Smela, E. 1999. Microfabrication of PPy microactuators and other conjugated polymer devices. *Journal of Micromechanics and Microengineering* 9:1–18.

Washizu, M., and Jones, T. B. 1996. Generalized multipolar dielectrophoretic force and electrorotational torque calculation. *Journal of Electrostatics* 38:199–211.

Washizu, M., Kurahashi, Y., Iochi, H., Kurosawa, O., Aizawa, S., Kudo, S., Magariyama, Y., and Hotani, H. 1993. Dielectrophoretic measurement of bacterial motor characteristics. *IEEE Transactions on Industry Applications* 29(2):286–294.

Wright, W. H., Sonek, G. J., Tadir, Y., and Berns, M. W. 1990. Laser trapping in cell biology. *IEEE Journal of Quantum Electronics* 26(12):2148–2157.